






## Open Archive Toulouse Archive Ouverte (OATAO)

OATAO is an open access repository that collects the work of Toulouse researchers and makes it freely available over the web where possible

This is an author's version published in: <http://oatao.univ-toulouse.fr/20292>

**Official URL:** <https://doi.org/10.1016/j.bioelechem.2013.09.006>

**To cite this version:**

Stipaničev, Marko  and Turcu, Florin and Esnault, Loïc and Rosas, Omar  and Basséguy, Régine  and Sztylek, Magdalena and Beech, Iwona B. *Corrosion of carbon steel by bacteria from North Sea offshore seawater injection systems: Laboratory investigation.* (2014) *Bioelectrochemistry*, 97. 76-88. ISSN 1567-5394

Any correspondence concerning this service should be sent to the repository administrator: [tech-oatao@listes-diff.inp-toulouse.fr](mailto:tech-oatao@listes-diff.inp-toulouse.fr)

# Corrosion of carbon steel by bacteria from North Sea offshore seawater injection systems: Laboratory investigation

Marko Stipanicev<sup>a,b,\*</sup>, Florin Turcu<sup>a</sup>, Loïc Esnault<sup>a</sup>, Omar Rosas<sup>b</sup>, Régine Basseguy<sup>b,\*\*</sup>, Magdalena Szttyler<sup>c</sup>, Iwona B. Beech<sup>c,d</sup>

<sup>a</sup> Det Norske Veritas, Johan Berentsens vei 109-111, 5163 Laksevåg, Bergen, Norway

<sup>b</sup> Laboratoire de Génie Chimique CNRS-INPT, Université de Toulouse, 4 Allée Emile Monso, 31030 Toulouse, France

<sup>c</sup> School of Pharmacy and Biomedical Sciences, University of Portsmouth, Michael's Building, White Swan Road, Portsmouth PO1 2DT, UK

<sup>d</sup> Department of Microbiology and Plant Biology, University of Oklahoma, 770 Van Vleet Oval, Norman, OK, USA

## ARTICLE INFO

### Keywords:

Seawater injection

Carbon steel

Corrosion

Bacterium

## ABSTRACT

Influence of sulfidogenic bacteria, from a North Sea seawater injection system, on the corrosion of S235JR carbon steel was studied in a flow bioreactor; operating anaerobically for 100 days with either inoculated or filtrated seawater. Deposits formed on steel placed in reactors contained magnesium and calcium minerals plus iron sulfide. The dominant biofilm-forming organism was an anaerobic bacterium, genus *Caminicella*, known to produce hydrogen sulfide and carbon dioxide. Open Circuit Potentials (OCP) of steel in the reactors was, for nearly the entire test duration, in the range  $-800 < E(\text{OCP})/\text{mV (vs. SCE)} < -700$ . Generally, the overall corrosion rate, expressed as  $1/(R_p/\Omega)$ , was lower in the inoculated seawater though they varied significantly on both reactors. Initial and final corrosion rates were virtually identical, namely initial  $1/(R_p/\Omega) = 2 \times 10^{-6} \pm 5 \times 10^{-7}$  and final  $1/(R_p/\Omega) = 1.1 \times 10^{-5} \pm 2.5 \times 10^{-6}$ . Measured data, including electrochemical noise transients and statistical parameters ( $0.05 < \text{Localized Index} < 1$ ;  $-5 < \text{Skewness} < -5$ ; Kurtosis  $> 45$ ), suggested pitting on steel samples within the inoculated environment. However, the actual degree of corrosion could neither be directly correlated with the electrochemical data and nor with the steel corrosion in the filtrated seawater environment. Further laboratory tests are thought to clarify the noticed apparent discrepancies.

## 1. Introduction

The economic consequences of corrosion of iron and its alloys in various industrial sectors, including oil and gas operations, are well documented [1–3]. Undisputedly, corrosion causes considerable damage to marine steel infrastructure, such as offshore oil installations and pipeline systems, leading to revenue losses. It has been estimated that nearly 20% of the total corrosion cost is due to Microbially Influenced Corrosion (MIC) [3,4]. MIC is often seen as pitting attack that is generally associated with the presence of surface-associated microbial communities embedded in a bioinorganic matrix, referred to as biofilm [5]. In both natural habitats and man-made systems, biofilms implicated in corrosion failures, comprise diverse microbial genera and species that often exhibit synergistic and syntrophic behavior [6,7]. Key microorganisms are phylogenetically diverse Sulfide-Producing Prokaryotes (SPP) of which some, but not all, represent Sulfate-Reducing Bacteria (SRB) and Archaea (SRA), i.e. Sulfate-Reducing Prokaryotes (SRP) [8,9]. In addition to SPP, Sulfur-Oxidizing Bacteria (SOB), Iron-Reducing

and -Oxidizing Bacteria (IRB and IOB respectively), Manganese-Oxidizing Bacteria (MOB), carbon dioxide reducing bacteria [3] and methanogenic archaea have been associated with marine corrosion failures [10–12].

It is now acknowledged that microbial metabolic activity, which depends on the availability of nutrients and of suitable electron donors and acceptors, can influence electrochemical processes on steel surfaces, therefore, plays an important role in the processes governing MIC [13,14]. Indeed, it has been reported that differences in metabolic activities within biofilms established under identical conditions can result in dissimilar corrosion rates [4]. It is also recognized that biofilm formation and associated MIC damage are dependent on the physical and chemical conditions of a given environment [15]. For example, temperature, pH, pressure, light radiation, oxygen content, salinity and redox potential will influence the nature and metabolic activity of a bacterial community [16], thus governing the potential risk of MIC. It is noteworthy that conditions at surfaces may differ significantly from those in bulk liquid; for example, anaerobic niches may exist within biofilm in a fully oxygenated system or oxygen may be formed in an anoxic environment due to bacterially-mediated disproportionation reactions [17–19].

Further, fluid flow directly impacts mass transfer and biofilm formation [20,21]. High shear stress is likely to decrease microbial

\* Correspondence to: M. Stipanicev, Det Norske Veritas, Johan Berentsens vei 109-111, 5163 Laksevåg, Bergen, Norway.

\*\* Corresponding author.

cell attachment and may even cause detachment of an established biofilm [21–23].

Importantly, the chemical composition and microstructure of the construction materials determine their susceptibility to both abiotic corrosion and MIC [24,25]. Carbon steel is a major alloy used in offshore oil extraction and transport systems, including Sea-Water Injection Systems (SWISs). During their operational lifetime, SWISs are exposed to a range of damage-provoking conditions. The presence of microorganisms can lead to complex, and not yet fully understood, deterioration of pipeline material. Carbon steel is particularly vulnerable to sulfide attack; hence biotic sulfide production resulting from SPP activity is of great concern.

In offshore Oil and Gas (O&G) industry, the main target in MIC control and remediation is taxonomically and metabolically diverse SRP. Able to grow within a wide temperature range, SRP are routinely detected in parts of the offshore oil extraction systems where sulfate-rich seawater-containing fluids are being produced or processed and anoxic conditions may prevail [26,27].

It has to be emphasized that not just SRP, but also other classes of anaerobic dihydrogen sulfide producing organisms, pose equal, if not greater, MIC threat [32]. These include spore forming bacteria belonging to the phylum *Firmicutes* and the class *Clostridia*, which are readily detected in oilfield systems using advanced molecular ecology techniques [28–31].

The interdisciplinary investigation reported herein aimed to determine whether the selection of S235JR low carbon steel as pipe material for a North Sea offshore seawater injection system would result in an unacceptable MIC risk. The laboratory set-up was constructed as an anaerobic continuous-flow bioreactor, circulating North Sea seawater. Its operating parameters were selected to mimic field conditions. The system was designed as a closed test loop comprising an inoculation vessel and two flow-through cells fitted with steel test specimens. Bioreactor inoculum was obtained from sessile (biofilm) field populations enriched in an anoxic sulfate medium and subsequently re-enriched in sulfate and other anaerobic microbial cultivation media. Special emphasis was placed on the on-line use of electrochemical techniques, in particular Linear Polarization Resistance (LPR) and Electrochemical Noise (EN), to monitor and characterize corrosion events on surfaces of steel specimens. The bioreactor inoculum and the planktonic and biofilm communities in the experimental and control flow cells were characterized employing tools of molecular microbial ecology, namely Polymerase Chain Reaction (PCR), Denaturing Gradient Gel Electrophoresis (DGGE), cloning and sequencing. Scanning Electron Microscopy (SEM) and Energy Dispersive X-ray (EDX) analysis of surfaces of test specimens were performed to image biofilms, visualize topography and to provide elemental composition of corrosion products.

## 2. Material and methods

### 2.1. The bioreactor loop

A high and stable flow rate of seawater, constant temperature, and anoxic conditions were prerequisites of the study. A closed flow-loop bioreactor design was selected as the most suitable system complying with those requirements. The final bioreactor set-up benefitted from the past 20-year experience in MIC research for the selection of construction materials, flow cell design, real-time monitoring techniques, etc. [33–36]. The main components of the bioreactor were manufactured in-house and comprise a vessel and two cylindrical flow-through cells. While the inoculated seawater freely enters the experimental flow cell, it passes through a 0.2 µm filter (Sartopore 2 MaxiCaps®, Sartorius AG, France) before reaching the control flow cell. The bioreactor set-up is depicted in Scheme 1.

The bioreactor vessel consists of a polypropylene body and an acrylic lid, fitted with an optical oxygen dipping probe, a temperature sensor interfaced with Fibox 3 fiber optic oxygen transmitter

(Presens, Germany), one nitrogen gas inlet (99.999% purity, YaraPraxiar, Norway), one gas outlet and a pH electrode (pH-meter HI-9125N, Hanna Norden AB, Sweden). The lid also incorporates an in-house fitted sampling point and a fluid injection system. The vessel is also equipped with a heating unit (ISOPAD IP-DASI®, Tyco, USA) and a thermostat (Raychem® AT-TS-14, Tyco Thermal Controls, USA).

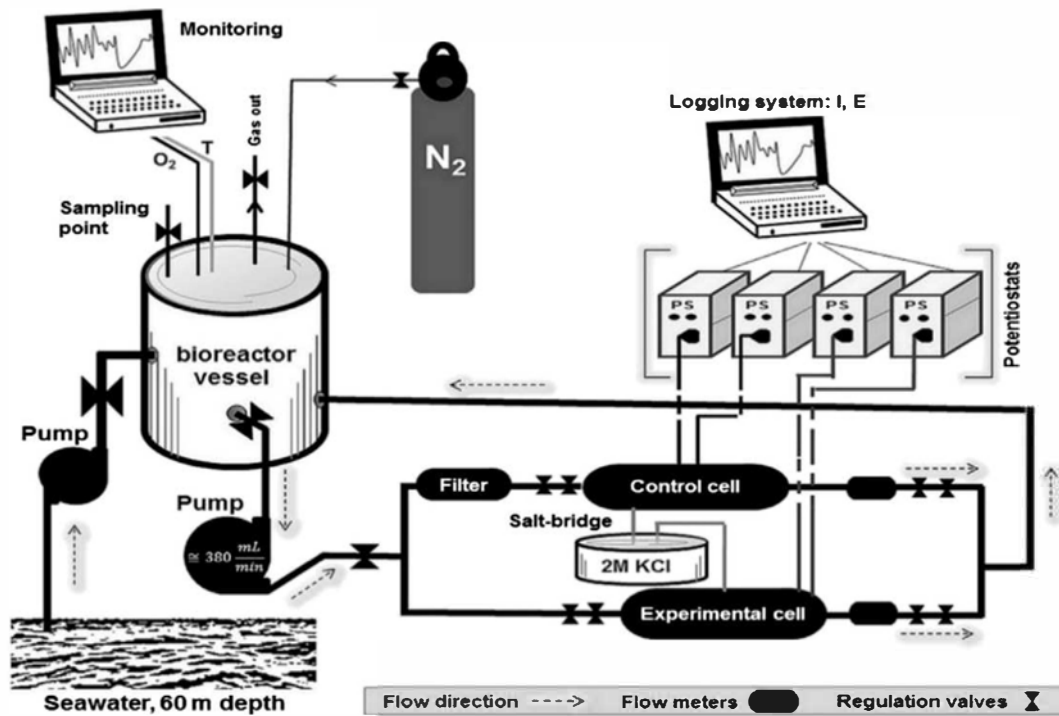
A peristaltic pump (W-M 520SN/REL, Watson-Marlow, UK), draws media from the bioreactor vessel, and the output flow is split between the two flow cells. Perfluoroalkoxy (PFA) tubing (PFA-T8-062-50, Swagelok, UK) was used. Two regulation needle valves (PFA-4RPS8, Swagelok, UK) were installed before and after each flow cell. Each flow cell was also equipped with a flow meter (FTB332 infra-red light beam micro-flow meter, Omega Engineering, UK) located after the exit regulation valve. The flow rate through each of the flow cells was controlled at 180 mL/min with the regulation valves. After passing through the flow cells, the liquid stream rejoins and returns to the bioreactor vessel. Liquids were re-circulated in the bioreactor loop for 100 days.

The entire bioreactor flow system was constructed from polymers to minimize contamination with exogenous metal ions. Furthermore, materials, including perfluoroalkoxy (2 mm thickness), polyolefin (1 mm thickness), polypropylene (2 cm thickness) and acrylic (1 and 2 cm thickness) polymers with minimal oxygen permeability and minimal deterioration under test conditions were chosen. Prior to operation the bioreactor loop was flushed with technical grade alcohol (art. no.601441, Kemetyl Norge AS, Norway) and flow cells were exposed for 6 h under UV light (XX-15 sterilization UV lamp, UVP, USA).

Flow cells were made from acrylic tubes (6 cm inner diameter, 1 cm wall thickness and 48 cm length). Six pairs of feedthroughs (M20 size fittings, produced by OBO Bettermann, Germany) were installed on each flow cell. A schematic drawing of a flow cell showing its cross section and distribution of feedthroughs is presented in Scheme 2.

Electrodes for the measurements of corrosion rates and open-circuit potentials were installed in the two flow cells, in identical arrangements. The electrode configuration was designed to reproduce that used in offshore electrochemical probes. Six carbon steel Working Electrodes (WE) with a circular, exposed area of 0.785 cm<sup>2</sup> (cylindrical specimens, 1 cm long, 1 cm diameter, dressed in polyolefin sleeve and leaving only the flat bottom of cylinder exposed, Scheme 3) were installed in the 10 o'clock (F2, F4, and F6) and 2 o'clock positions (F8, F10, and F12), see Scheme 2. Each cell was also fitted with four additional electrodes. Their design was the same as that of the working electrodes (Scheme 3), except that Inconel® C276 (*E*(Inconel®C276 in anoxic seawater)/mV (vs. SCE) ≈ 350) was used instead of carbon steel as electrode material and the exposed area was 3.95 cm<sup>2</sup> as the cylinder side was not dressed in polyolefin sleeve. Two of these electrodes, installed in the F5 and F9 positions, were used as Counter Electrode (CE). The other two, installed in the F3 and F11 positions, served as Pseudo-Reference Electrodes (PRE). Two laboratory-made Salt-Bridges (SB) filled with 2 M KCl solution (VWR, US) were placed between the F1 position in each flow cell and a reference cell, which was also filled with the 2 M potassium chloride solution and fitted with two Saturated Calomel Electrodes (SCE). An in-house manufactured liquid Sampling Port (SP) with a septum was installed at F7 position in each cell. To monitor biofilm formation, five carbon steel specimens (half-pipe sections with a 5 cm length, a 5.5 cm outer diameter and a 0.5 cm wall thickness) were installed at 6 o'clock position in each flow cell (Scheme 2).

The test specimens (half-pipe and circular disks) were manufactured from S235JR carbon steel (Descours and Cabaud, France). The S235JR carbon steel is composed of the following elements and corresponding mass percentage: 0.17% carbon (C), 1.4% manganese (Mn), 0.045% copper (Cu), 0.03% sulfur (S) and 0.03% phosphorus (P). All exposed surfaces were ground manually using silicon carbide (SiC) paper of increasingly fine grain, ending with 600-grit. Grinding debris were rinsed off the electrode surface with sterile deionized water.



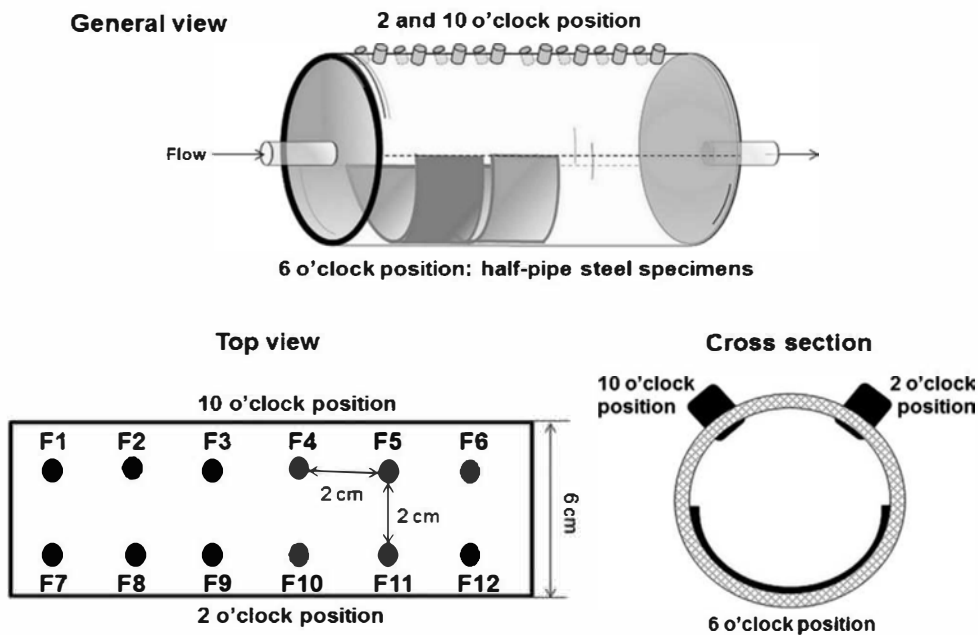
Scheme 1. Schematic representation of the bioreactor loop.

The specimens were exposed for 3 h on each side under UV light (wave length 256 nm: XX-15, sterilization UV lamp, UVP, USA) at 25 °C.

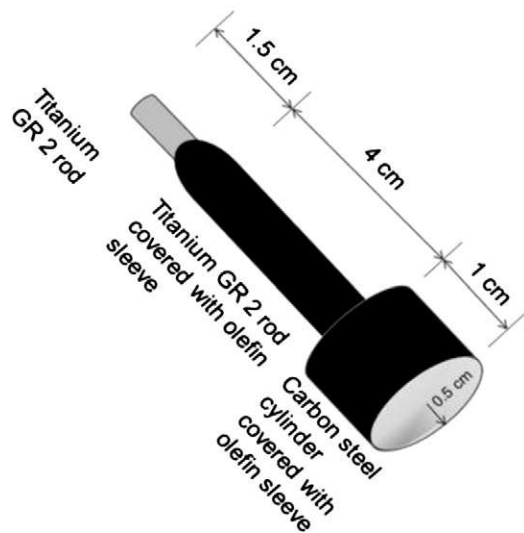
The bioreactor vessel was filled up with 40L of seawater, and oxygen was removed by purging with nitrogen for 3 days, i.e. until the optical oxygen probe reached its detection limit of 10 ppb. The flow system was then activated, and the flow rate maintained at 180 mL/min in each of the flow cells for the initial 15 days of the test. 15 days after the start of the test flow was stopped for 2 days, and the bioreactor vessel was seeded with bacterial inoculum. Then flow was re-established.

The bioreactor loop was operated continuously for the next 83 days. At the end of the 100-day period, the reactor was decommissioned. Electrochemical measurements were carried out at regular intervals, as described in Section 2.2.

Microbial consortia which served as a source of inoculum for the laboratory bioreactor loop were obtained from a SWIS located on an off-shore installation, code name S, in the Norwegian sector of the North Sea. Two bio-probes (0.3 cm<sup>2</sup> surface area with 0.08 cm in diameter and a length of 1.2 cm) manufactured from St-52 carbon steel were removed from a SWIS side-stream rig after one and three months of



Scheme 2. Schematic representation of cross-section and fitting distribution of the flow through cell.



Scheme 3. Working electrode scheme.

exposure, respectively, following the offshore procedure API-RP 39 for handling biological samples [37]. Upon removal, the bio-probes were immersed in 50 mL of sterile SRB/2 growth-medium (Commercial Microbiology, UK) and subjected to 20 s of sonification (UltraMet® 2005 Sonic Cleaner, Buehler, US). Following sonification, 1 mL volumes of biofilm suspensions were inoculated aseptically into six glass vials, each containing 9 mL of deoxygenated sterile SRB/2 medium. The vials/cultures were incubated on site at 20 °C for 28 days, after which period enumeration of viable bacterial cells was carried out using Most Probable Number (MPN) method. Cultivation of biofilms retrieved from one and three month-exposed bio-probes in SRB/2 growth medium resulted with cell densities of 43 cells/mL and >1100 cells/mL respectively. The 28-day-old SRB/2 enrichments were subsequently used for inoculating a range of anaerobic liquid media, as specified below.

1. Seawater + iron dust (3 g/50 mL)
2. Seawater + SL-10 trace elements solution
3. Seawater + acetate (10 mM) + SL-10
4. Seawater + acetate (10 mM) + Iron dust (3 g/50 mL) + SL-10
5. SRB/2 medium

SL-10 trace element solution is used in the preparation of Widdel medium as described elsewhere [38].

The resulting re-enrichments were incubated for 21 days as described above. Following incubation, all re-enrichments were combined to produce the Bioreactor Vessel Inoculum (BVI) of a total volume of 1.5 L. Prior to bioreactor seeding iron was removed from the inoculum using a strong magnet.

## 2.2. Analytical methods

### 2.2.1. Electrochemical methods

The Open Circuit Potential (OCP), e.g.  $E/(OCP)/mV(vs. SCE)$ , measurements were performed with a 34401A  $6^{1/2}$  digit multimeter with an input impedance of 10 G $\Omega$  in parallel with 100 pF (Agilent, USA). The  $E/(OCP)/mV(vs. SCE)$  of three working electrodes (circular disk) installed at the F4, F6 and F12 positions of each flow cell were recorded every 3 days.

The Linear Polarization Resistance (LPR) and Electrochemical Noise (EN) measurements were carried out using a multichannel potentiostat MultEchem™ (Gamry Instruments, USA) that consisted of two Reference 600TM Potentiostat/Galvanostat/ZRA independent units

connected to a PC interface and monitored with DC105 and ESA410 software (Gamry Instruments, USA). The LPR technique was employed to estimate the rate of corrosion of the steel WEs. The polarization resistance ( $R_p$ ) of the steel/electrolyte interface is measured in the vicinity of the  $E(OCP)$  and is given in  $\Omega$  [39,40].  $R_p/\Omega$  is defined as the slope of the polarization curve tangent at the  $E(OCP)/V$ . The inverse of  $R_p$  is proportional to the “instantaneous” corrosion rate and given in  $1/\Omega$  [15]. To determine  $R_p/\Omega$ , the potential was scanned in the range of  $+20 > E(OCP)/mV > -20$  (with  $E(OCP)$  measured using 600TM Potentiostat) and a sweeping rate of  $v/(mV/s) = 0.167$ . Polarization scans were performed every 14 days during the first 91 days and every day during the last 9 days of the test.

Standard three electrode-arrangements included a WE, a CE and of a PRE. Three different electrode configurations were used:

- 1) WE at F8, 2 o'clock, CE at F9, 2 o'clock, and PRE at F3, 10 o'clock;
- 2) WE at F4, 10 o'clock, CE at F5, 10 o'clock, and PRE at F11, 2 o'clock;
- 3) WE at F10, 2 o'clock, CE at F9, 2 o'clock, and PRE at F3, 10 o'clock.

Averages ( $1/R_p$ )-values with associated standard deviations were reported for the three different working electrodes.

Electrochemical Noise (EN) analysis was carried out to determine the type of corrosion attack [41,42]. Electrochemical Current Noise (ECN) and Electrochemical Potential Noise (EPN) signals were recorded between two equivalent working electrodes (placed at F6 and F12) using a PRE at F11. Here presented ECN and EPN data were recorded with data sampling rates of 0.1 Hz, 0.2 Hz and 1 Hz, a current range of 600 mA, a potential range of  $+/-3$  V, a current resolution of 1 pA and a voltage resolution of 1  $\mu V$ . Data sampled at 0.1 Hz were collected continuously for the whole testing period of 100 days; data sampled at 1 Hz were collected at four different 2-day time periods; while data sampled at 0.2 Hz were recorded for a 2-day period at the beginning of the test, prior to reactor inoculation.

Due to equipment problems, no EN data were recorded between day 69 and day 72 for either flow cell. Data was also not recorded between test start and day 6 and day 18 and day 24 for the experimental cell.

EN data sampled at 0.1 Hz were analyzed in the sequence-independent domain within data blocks of 128 sampling data points, and thus the time resolution for each calculated statistical parameter is 21.3 min. Dimensionless statistical parameters such as Localization Index (LI), skewness and kurtosis were calculated [41–43]. They can all be presented as indicators of localized corrosion activity [41–43]. Localization index (LI) was calculated as the ratio between the ECN standard deviation ( $\sigma_{iECN}/A$ ) over the root-mean-square current value ( $I_{rms}/A$ ) [41]. The analysis took into account the different ranges of LI values, which lie between 0 and 1. Skewness was derived as the ECN third central moment ( $m_{3,ECN}/A$ ) divided by the cube of the ECN standard deviation ( $\sigma_{iECN}/A$ ). Kurtosis was derived by dividing the ECN fourth central moment ( $m_{4,ECN}/A$ ) by the fourth power of the ECN standard deviation ( $\sigma_{iECN}/A$ ).

Modulated current and potential signal patterns, as well as transients, characteristic of localized surface events, were visually examined within data blocks of 100 (0.1 Hz sampling frequency), 200 (0.2 Hz sampling frequency) and 1000 (1 Hz sampling frequency) points resulting with the time resolution of 1000 s.

### 2.2.2. Surface analysis

After reactor decommissioning, the topography of all working electrodes was characterized using optical imaging with a Leica upright DMR microscope (Leica Microsystems GmbH, Germany) and attached ProgRes® C5 camera (JENOPTIK Optical Systems GmbH, Germany). Prior to examination, steel specimens were cleaned from corrosion products by immersion in a 5 (w/v)% hexamine (MERCK, Germany) solution in concentrated hydrochloric acid (VWR, USA) for 30 s. This was immediately followed by rinsing with deionized water, gentle blotting with a paper towel, and overnight storage in a desiccator.

Four half-pipe steel specimens, two from each flow cell, were removed from the bioreactor and equally divided into two batches. Specimens were prepared for Scanning Electron Microscopy (SEM) analysis as follows:

- a) Batch No. 1: specimens were dried under nitrogen stream and immediately examined with the high resolution SEM (JSM-5800, Joel, Japan) interfaced with a EDX acquisition system (Voyager®, NORAN Instruments Inc., USA)
- b) Batch No. 2: specimens were placed in 2.5 (w/v)% glutaraldehyde (Electron Microscopy Science, USA) for 90 min at 4 °C and then surface deposits were removed by sterile scalpel blade. Biofilm samples were washed by 4 × 15 min immersions in 0.1 M sodium cacodylate buffer (MERCK, Germany). Post-fixation was carried out by placing biofilm samples for 1 h in the solution of 1 (w/v)% osmium tetroxide (purity > 99.95%, Electron Microscopy Science, USA) in 0.1 M sodium cacodylate buffer. Post-fixed samples were washed in 0.1 M sodium cacodylate buffer (2 × 20 min) and dehydrated following serial immersions (15 min in 30 (v/v)%, 15 min in 50 (v/v)%, 20 min in 70 (v/v)%, 2 × 15 min in 96 (v/v)% and 2 × 15 min in 100 (v/v)% in aqueous ethanol (99.8%, Sigma-Aldrich, Norway) solutions). De-watered biofilm samples were placed in an oven (Type TS 4057, Thermaks AS, Norway) at 37 °C overnight. Dried samples were sputter-coated with palladium for 6 min and imaged with high resolution SEM (JSM-7400F, Joel, Japan).

All EDX results are given as percentage by number of atoms (At(element)/%) of each of the elements identified in scanned area.

### 2.2.3. Elemental analysis

A representative part of corrosion products was removed from the surface of one steel half-pipe specimen from each flow cell. Each specimen was placed for 1 h in 20 mL of filtered (0.22 µm) aqueous hydrochloric acid solution (50 (v/v)%), and stored at 4 °C for further analysis. Iron and major seawater cations (sodium (Na), calcium (Ca), magnesium (Mg) and potassium (K)) and anions such as sulfur (S) and phosphorus (P), were analyzed with Inductively Coupled Plasma-Atomic Emission Spectroscopy (ICP-AES) (Ultra-trace 2000 ICP-AES, Jobin Yvon®, Horiba, Japan).

All ICP-AES results are shown as molar concentrations (c(element)/mM).

### 2.2.4. Microbiological diversity assessment

The following samples were used for deoxyribonucleic acid (DNA) analysis:

1. As-received North Sea seawater (SW)
2. The biofilm field enrichment in SRB/2 medium (BFE)
3. Bioreactor vessel inoculum consisting of pooled re-enrichments as described in section 2.4.1 (BVI)
4. Biofilms removed from steel specimens exposed in the control flow cell (BCFC)
5. Biofilms removed from steel specimens exposed in the experimental flow cell (BEFC)
6. Water samples from the experimental flow cell (WEFC)

Total DNA was isolated from each sample using the PowerBiofilm™ DNA isolation kit (Mo BIO Laboratories, UK) according to the manufacturer's instructions. The concentration of extracted and purified DNA was determined using a NanoDrop ND-1000 spectrophotometer (Thermo Scientific, USA). All extracted DNA was stored at -20 °C.

Isolated DNA was subject to Polymerase Chain Reaction (PCR) (peqStar 96 Universal Gradient, PeqLab, UK). The 16S rRNA gene (550 bp) was amplified using universal bacterial primers: 341 F + GC (5'-CGC CCG CCG GCG GCG GCG GCG GCG GCA CGG GCG GCC TAC GGG AGG CAG CAG-3') and 907R (5'-CCG TCA ATT CMT TTG AGT TT-3) [44] (Life Technologies, UK). PCR reactions were performed in 50 µL mixtures, containing 25 µL of 10× GoTaq® Green Master Mix

(Promega, UK) and 1 µL of each primer (10mM). The DNA was initially denatured at 94 °C for 4 min; followed by a touchdown PCR: 20 cycles of 94 °C for 1 min, 63–54 °C for 1 min and 72 °C for 1 min followed by 15 cycles of 94 °C for 1 min, 53 °C for 1 min and 72 °C for 1 min with a final 10-minute cycle at 72 °C. The PCR products were separated on a 1.0% agarose gel stained with SYBR® Safe DNA gel stain (Invitrogen Corp., USA) and viewed under UV transillumination (Alpha Innotech Corporation, USA) and Digital Camera (Olympus C-4000 Zoom) to ensure that the correct size fragment was amplified.

PCR-amplified bacterial 16S rRNA gene products (30–40 µ) were separated by Denaturing Gradient Gel Electrophoresis (DGGE) using an Ingeny DGGE apparatus (Ingeny International BV, The Netherlands), at the temperature of 60 °C for 20 h. The voltage was set to 90 V, after an initial 10 min at 200V. The standard gradient was formed of 6% polyacrylamide in 0.5 × Tris-acetate-EDTA (TAE) buffer with between 30% and 80% denaturant (7 M urea and 40% formamide defined as 100% denaturant). Following electrophoresis, the gel was stained with SYBR® Safe DNA gel stain (Invitrogen Corp., USA), viewed under UV transillumination and a permanent image captured using the Alpha Innotech Gel Documentation System (Alpha Innotech Corporation, USA).

All visible bands were cut from the gel using a sterile scalpel blade. To extract the DNA, each cut-out was transferred into sterile 1.5 mL microcentrifuge tubes containing 30 µL of ultra-pure water and then centrifuged at 13,000 g for 1 min (Heraeus Fresco 21, Thermo Scientific, UK). Aliquots (5 µL) of supernatants were used for PCR re-amplification as described above. PCR products were purified with the NucleoSpin® Extract II PCR purification kit (Macherey-Nagel, UK) and sequenced by GATC Biotech (UK).

PCR-amplicons were cloned into the pGEM-T Easy Vector (Promega, UK) according to standard methods [45]. *Escherichia coli* JM 109 (Promega, UK) was used as a host strain for molecular cloning [46]. *E. coli* JM 109 was grown in Lysogeny Broth (LB) medium [45] and Super Optimal Broth with Catabolite repression (SOC) medium (Promega, UK) at 37 °C. The solid LB medium was supplemented with 100 µg/mL ampicillin, 100 µg/mL X-Gal and 0.5 mM IPTG. Recombinant plasmid DNA was purified using a NucleoSpin® Plasmid QuickPure (Macherey-Nagel, UK) following the manufacturer's instructions.

Recombinant plasmid extraction and purification was carried out from liquid cultures of the positive *E. coli* colonies obtained from the transformation using NucleoSpin® Plasmid QuickPure (Macherey-Nagel, UK) following the manufacturer's protocol (Plasmid DNA Purification User Manual, 07/2010 p.18–19).

Purified plasmids were sent to the GATC Biotech UK DNA sequencing service. Bacterial identification was carried out through sequence homology searches in Basic Local Alignment Search Tool (BLAST).

## 3. Results

### 3.1. Evaluation of electrochemical data

Prior to bioreactor seeding, OCPs for working electrodes (circular disks) in both the control and experimental flow cells fluctuated between  $-950 < E(\text{OCP})/\text{mV}$  (vs. SCE)  $< -710$  (Fig. 1). Following inoculation OCPs stabilized at  $-800 < E(\text{OCP})/\text{mV}$  (vs. SCE)  $< -700$  in both flow cells.

Prior to bioreactor seeding, average  $1/(R_p/\Omega)$  values of approximately  $2 \times 10^{-6}$  were recorded for specimens in the control cell (Fig. 2). Between day 24 and day 52, average  $1/(R_p/\Omega)$  values increased to approximately  $1.1 \times 10^{-5}$  but with relatively large fluctuations. During the subsequent 27 days of the test,  $1/(R_p/\Omega)$  decreased to  $4.5 \times 10^{-6}$  and from day 79 until the test termination  $1/(R_p/\Omega)$  gradually increased and reached a final value of  $1.1 \times 10^{-5}$ .

Values of  $1/(R_p/\Omega)$  for steel coupons in the experimental flow cell are shown in Fig. 2. Preceding inoculation,  $1/(R_p/\Omega)$  values were similar to the ones recorded in the control cell. Following inoculation,  $1/(R_p/\Omega)$  increased gradually from  $2 \times 10^{-6}$  at day 24 to  $5 \times 10^{-6}$  at day 52 and

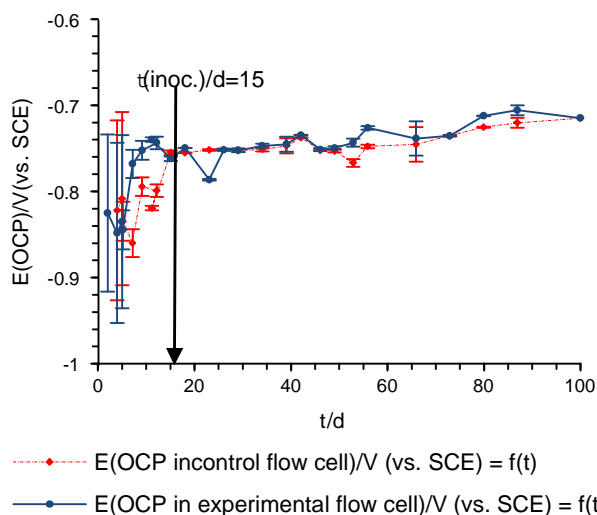


**Fig. 1.** Open circuit potential of S235JR carbon steel ( $E(\text{OCP})/\text{mV}(\text{vs. SCE})$ ) versus time ( $t/\text{d}$ ) obtained from steel specimens exposed in control (dashed line) and experimental (full line) cell during the 100 days. Data points are accompanied with standard deviation error bars.

then remained relatively stable for the next 25 days. After approximately day 77 strong increase in  $1/(R_p/\Omega)$  from  $5 \times 10^{-6}$  to approximately  $2 \times 10^{-5} \Omega^{-1}$  was measured, and during the last 6 days of exposure,  $1/(R_p/\Omega)$  values gradually decreased to  $1.2 \times 10^{-5}$ .

### 3.1.1. Corrosion monitoring using real-time EN data acquisition and time records analysis

An ECN (and associated EPN) transient, representative of those observed in the control during the initial 24 days of the test, i.e. prior to and just after inoculation, is presented in Fig. 3A. The modulated current and potential signals are indicative of pitting corrosion [47,48]. Briefly, the rapid current increase during pit initiation and growth is followed by a slower decay after pit repassivation.

Examples of 1000-second ECN and EPN time records, representative of those observed in the control flow cell between day 24 and day 100 are presented in Fig. 4A. Displayed examples were recorded at day 37, day 83 and day 100, with an acquisition frequency of 1 Hz. The ECN and EPN fluctuations are not characteristic of stable localized corrosion. Instead, transients related to metastable pitting and higher localized electrochemical surface activities of carbon steel were observed [48].

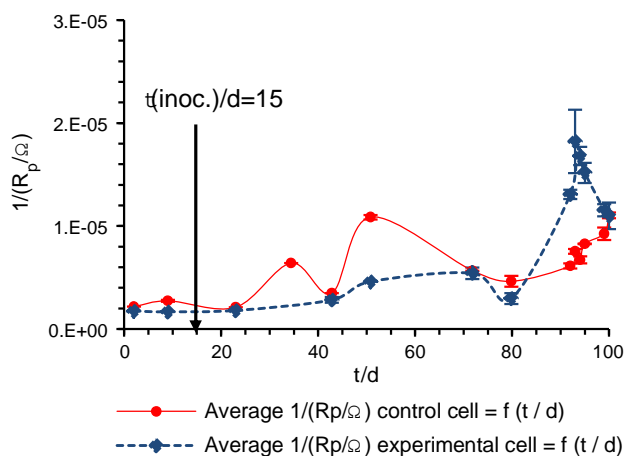


**Fig. 2.** Average instantaneous corrosion rate ( $1/(R_p/\Omega)$ ) with standard deviation error bars versus time ( $t/\text{d}$ ) in the control cell (full line) and experimental cell (dashed line) obtained by LPR technique during the 100 days.

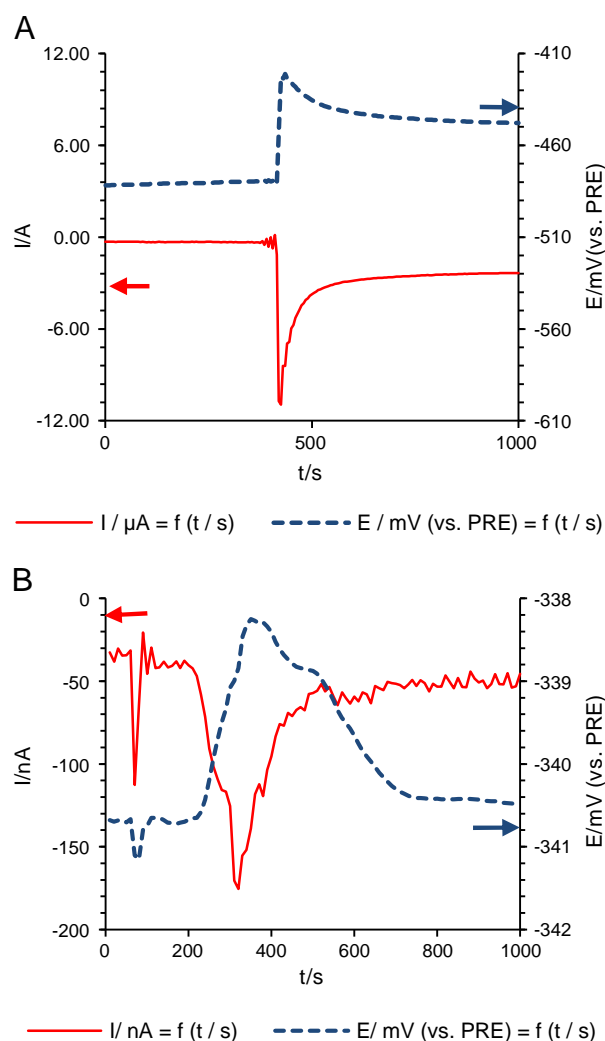


**Fig. 3.** (A) Typical current time record ( $I/\mu\text{A} = f(t/s)$ ) and potential time record ( $E/\text{mV}(\text{vs. PRE}) = f(t/s)$ ), sampled with 0.2 Hz frequency in the control cell during initial 19 days of the test; (B) typical current time record ( $I/\text{nA} = f(t/s)$ ) and potential time record ( $E/\text{mV}(\text{vs. PRE}) = f(t/s)$ ), sampled with 0.1 Hz frequency in the experimental cell during initial 19 days of the test.

The data maintained the same pattern throughout testing period, which would suggest combined uniform and localized attack.

In the control cell, ECN fluctuation with time had a tendency towards high values (higher currents) that corresponds to rise in  $1/(R_p/\Omega)$  values, especially in the last period of the test.

An ECN (and associated EPN) transient, representative of those observed in the experimental cell prior to and just after inoculation, during the entire initial 24 days of testing is presented in Fig. 3B. Shape of current and potential signals was very similar to ones observed in control cell. Moreover, fluctuation pattern i.e. transients observed in experimental flow cell between day 24 and day 100 were almost identical to ones observed in control flow cell as show in Fig. 4B (displayed records were collected at day 37, day 83 and day 100, with an acquisition frequency of 1 Hz).

### 3.1.2. Corrosion mechanism monitoring by EN sequence independent analysis

Localized Index (LI) values obtained from the sequence-independent analysis of ECN data from the control cell are presented in Fig. 5A. With one LI data point calculated for every 1280 s (about 21.3 min), fluctuations between 0.005 and 1 were observed during the initial 24 days.

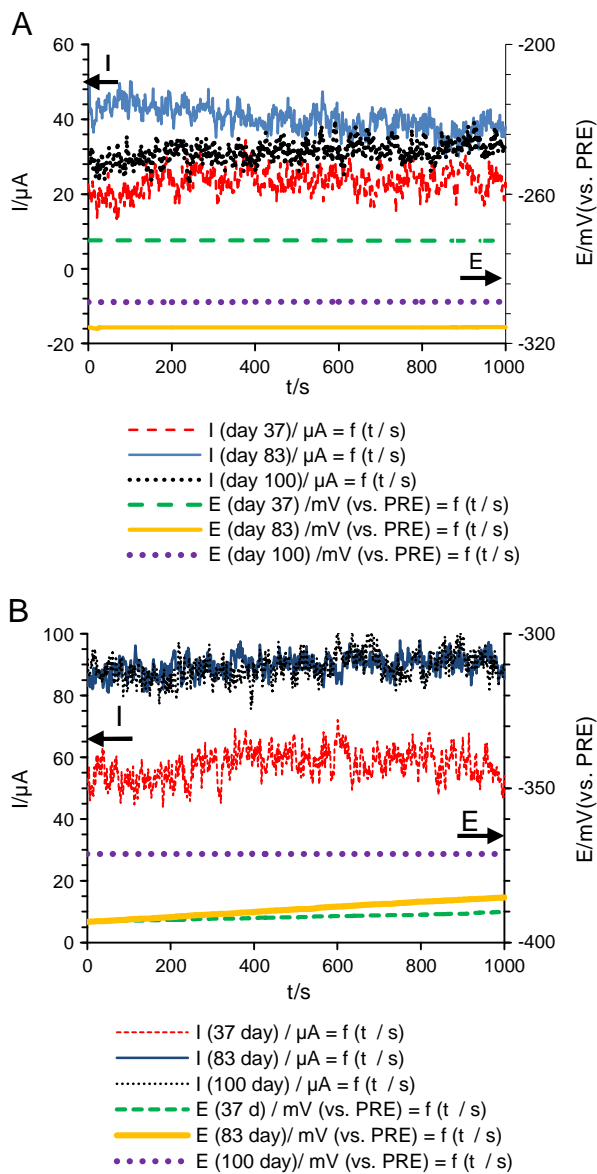


**Fig. 4.** Typical current time record ( $I/\mu\text{A} = f(t/s)$ ) and potential time record ( $E/\text{mV}(\text{vs. PRE}) = f(t/s)$ ), sampled with 1 Hz frequency during the period from day 24 of the test until the test termination: (A) Control cell; (B) experimental cell.

Higher values of LI can be interpreted as increased surface electrochemical activity that could be correlated with the tendency for localized reactions [47], what is in agreement with observed characteristic current and potential trends (Fig. 3A).

The fluctuations of LI correspond to localized corrosion and metastable pitting/uniform corrosion common for low carbon steel in a marine environment [42]. After 30 days, the initial LI decreased to values around 0.1 and it was maintained in that range. Since LI values do not correspond to values characteristic of general corrosion or to any other type of corrosion, they can, therefore, be interpreted as indicative of mixed corrosion [49]. It is likely that the continuous initiation, activation and de-activation of numerous pits resulted in general corrosion.

LI values obtained from the sequence independent analysis of ECN data from working electrodes exposed in the experimental flow cell are presented in Fig. 5B. Compared to data obtained from the control cell, the LI values are much smaller. During the first 19 days, the fluctuations of LI occurred mainly in the range from 0.005 to 0.05 with occasional and random increases to a value of 1. Most likely, the localized corrosion activity was low and uniform corrosion dominated [48].

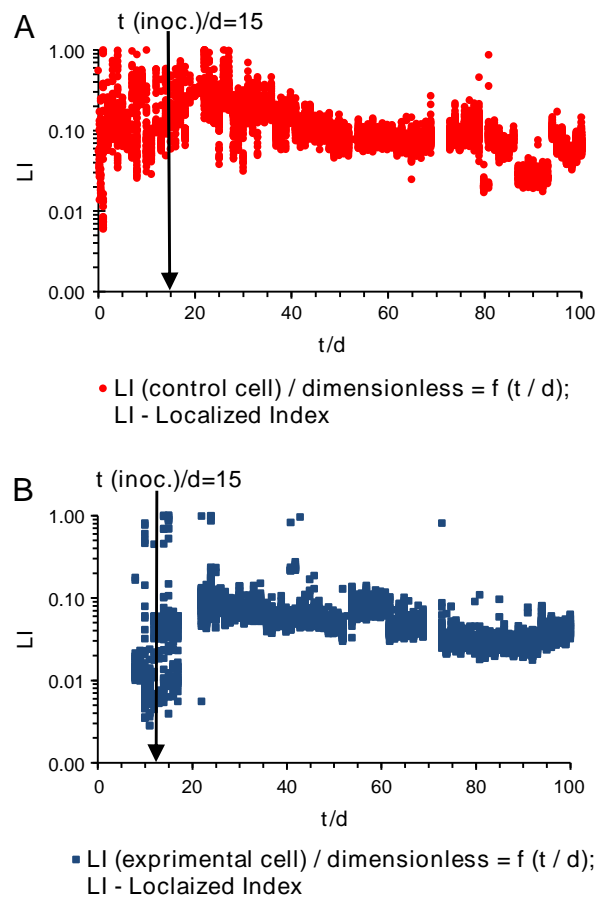


**Fig. 5.** Localized Index (LI/dimensionless) values calculated for ECN data acquired in the control cell, versus time ( $t/d$ ), during the 100 days test period for: (A) Control cell; (B) experimental cell. All calculated points plotted (67 point/day).

Furthermore, during the same time period, LI fluctuations up to a value of 1 were noted. This corresponds to transients that were observed during the analysis of current and potential records and which were indicative of pitting (Fig. 3). After 22 days an increase in LI from approximately 0.02 to 0.1 was recorded. It is likely that the prevailing boundary and/or mixed corrosion resulted from the initial metastable pitting attack, which led to uniform corrosion.

Furthermore, acquired ECN data were subjected to additional statistical analysis resulting in calculation of skewness and kurtosis values. Fig. 6A reveals that for WE in the control cell, the skewness fluctuated in the range  $-0.6 < \text{skewness} < 0.6$  and kurtosis in the range  $-1.2 < \text{kurtosis} < 1.2$  for most of the duration of the test. Larger fluctuations of skewness (up to a value of 5) and of kurtosis (up to a value of 20) were detected mainly during the initial 22 days of testing. For both parameters, values within a range of  $-1 < \text{skewness}$  and  $\text{kurtosis} < 1$  indicate uniform corrosion [43]. The result thus suggests that this type of corrosion was dominant in the control flow cell. However, randomly occurring higher values of kurtosis signify the presence of sporadic localized surface events.

In the experimental flow cell, skewness and kurtosis values were mostly in the range of  $-1 < \text{skewness}$  and  $\text{kurtosis} < 1$  (Fig. 6B). Larger fluctuations of skewness,  $-5 < \text{skewness} < 5$  and of kurtosis (up to value of 45) were occasionally observed, in particular during the initial 18 days of the test. The higher value of skewness and kurtosis coincided with higher values of LI. However, even the maximum recorded values fell within the range attributed to uniform corrosion [47]. Although initial fluctuations of skewness and kurtosis were more pronounced in the experimental cell, the general behaviors of these two parameters were



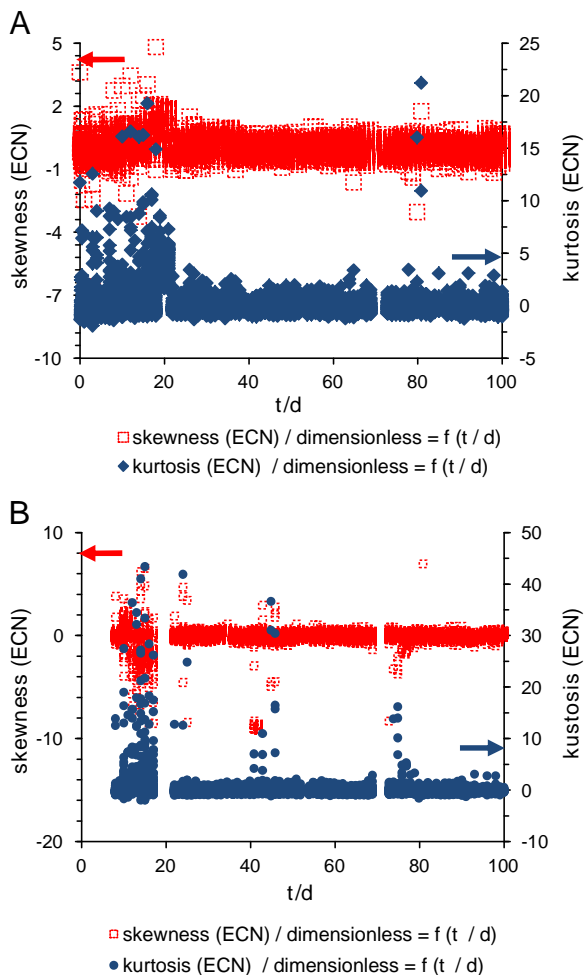


**Fig. 6.** Skewness (ECN)/dimensionless and kurtosis (ECN)/dimensionless values calculated for ECN data acquired during the 100 days versus time ( $t/d$ ): (A) Control cell; (B) experimental cell. All calculated points plotted (67 point/day).

rather similar for the two cells during the testing period and indicative of general corrosion.

### 3.2. Surface analysis

SEM micrographs revealed differences in morphology and abundance of deposits on steel specimens located at the 6 o'clock position in the control and experimental cells. In the latter flow cell, abundant black deposits were seen (Fig. 8A), while only scarce greenish deposits were noted in the control cell (Fig. 7A). The presence of biofilms was

evident in SEM micrographs depicting surfaces of specimens exposed in the experimental cell (Fig. 8B). There was no visible biofilm on surfaces of specimens in the control cell (Fig. 7B).

EDX analysis (Table 1) revealed the presence of iron (Fe), sulfur (S), oxygen (O), magnesium (Mg), calcium (Ca) and chlorine (Cl) in corrosion products on surfaces of steel specimens irrespective of the exposure conditions. However, their atomic fractions for scanned surfaces (At%), differed between the flow cells. The elemental composition was independently confirmed using ICP-AES analysis of dissolved corrosion products (Table 2). The amount of sulfur was statistically significantly higher in corrosion products on surfaces of samples exposed in experimental flow cell. Although EDX cannot provide direct information on the identity of the compound associated with the sulfur peak, the observation of the iron signal in the spectra together with sulfur peak supports that the black deposits, that when exposed to hydrochloric acid produced smell characteristic of sulfide, observed on specimens in the experimental cell (Fig. 8A) were iron sulfides. Bacterial cells imaged on surfaces of these specimens were associated with crystalline structures (Fig. 8B). Spectra of specimens exposed in both the control and experimental cells revealed high levels of calcium and magnesium (Tables 1 and 2). Both chlorine and oxygen peaks were also prominent in these deposits. Although speculative, it is not inconceivable that under ambient temperature conditions biominerals such as e.g. green rusts I and II (Fe(II) Fe(III) hydroxycarbonate, or hydroxysulphate, respectively) or dolomite ( $\text{CaMg}(\text{CO}_3)_2$ ) were formed [50,51]. In marine environments, green rust is often identified as a carbon steel corrosion product. The green rust formation could explain visual observations of faint green deposits on surfaces of the specimens from the control cell (Fig. 7A). Although such deposits were not seen on surfaces of specimens from the experimental cell (Fig. 8A), corrosion product analysis (Table 2) indicated that these minerals are likely to be present. The absence of biofilms on specimens exposed at 6 o'clock position in the control cell was reflected by the different chemical composition of the corrosion products, (low sulfide concentration) and the absence of black deposit (Fig. 7A and B). In addition to being present in dolomite, the calcium peak in EDX spectra is probably also associated with calcium carbonate, most likely aragonite. The long crystal rod seen in SEM micrograph (Fig. 7C) is similar to the reported structure of this mineral [52].

The removal of corrosion products from specimen surfaces exposed the general corrosion pattern (Fig. 9).

### 3.3. Characterization of bacterial communities

Five 16S rRNA libraries were generated using DNA isolated from samples listed in Section 2.2. The recovery of DNA from biofilms removed from steel surfaces exposed in the control flow cell (BCFC) and from water collected from this cell (WCFC) which would provide meaningful sequences was unsuccessful. The total number of bands in DGGE

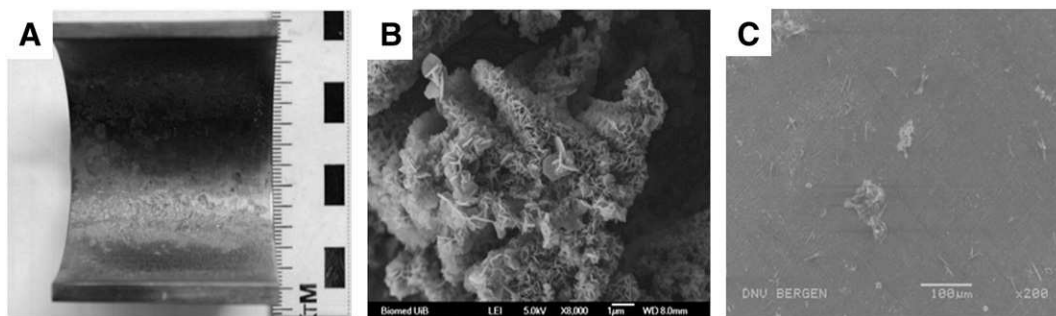


**Fig. 7.** Macro and micro photographs (6 o'clock position) of specimens after 100 days of a exposure in the control cell: (A) Photograph of coupon before preparation for SEM/EDX; (B) SEM image (8000 $\times$ ) of the immobilized corrosion products deposits; (C) SEM image (200 $\times$ ) of gray/greenish layer formed in the coupon, total area is scanned by EDX.

**Table 1**  
Results of EDX surface analysis of 6 o'clock coupons after 100 days of exposure in control and experimental cell. Results given in atomic fractions (At(element)/%) for iron (Fe), sulfur (S), oxygen (O), magnesium (Mg), calcium (Ca) and Chlorine (Cl).

	At(Fe)/% <sup>a</sup>	At(S)/% <sup>b</sup>	At(O)/% <sup>c</sup>	At(Mg)/% <sup>d</sup>	At(Ca)/% <sup>e</sup>	At(Cl)/% <sup>f</sup>
Control cell – corrosion product	49.2	1.8	33.8	1.9	0.1	3.3
Control cell – surface after corrosion product removing	80.3	0.3	8.7	NA	0.1	0.1
Experimental cell – corrosion product	31.5	5.2	48.6	0.7	0.3	9.9
Experimental cell – surface after corrosion product removing	89.0	0.7	8.4	NA	NA	NA

<sup>a</sup> Percentage of iron (Fe) by number of atoms in the scanned area.

<sup>b</sup> Percentage of sulfur (S) by number of atoms in the scanned area.

<sup>c</sup> Percentage of oxygen (O) by number of atoms in the scanned area.

<sup>d</sup> Percentage of magnesium (Mg) by number of atoms in the scanned area.

<sup>e</sup> Percentage of calcium (Ca) by number of atoms in the scanned area.

<sup>f</sup> Percentage of chlorine (Cl) by number of atoms in the scanned area.

profiles in samples with recoverable intact DNA (profiles not shown) is summarized in Table 3.

DGGE analysis of the seawater sample (SW) revealed 11 unique bands in DNA profile, which indicates the presence of at least 11 different bacterial strains. None of the bands detected in SW could be matched with bands obtained from field enrichments (BFE) or from the bioreactor vessel inoculum (BVI). DNA profile from BVI revealed 7 bands of which 4 were shared with the profile representing biofilms removed from steel specimens exposed in the experimental flow cell (BEFC). This strongly suggests that out of at least 7 strains seeded into the bioreactor vessel only 4 were successful in colonizing steel surfaces. At least 2 bands in BEFC profile originated from SW as they were absent from BVI profile. All 4 bands seen in the profile of DNA which represented planktonic population in the experimental cell (WEFC) were common with bands seen in BVI and BEFC profiles. Thus, at the time of sampling, 2 out of 6 bacterial strains detected in BEFC were present solely as sessile populations and were not detectable in the bulk liquid phase. The DNA profile from the biofilm field enrichment in SRB/2 medium (BFE) was the least divers with only 3 visible bands, all of which were represented in BEFC profile.

Three very faint bands were observed in DGGE profiles of DNA from bulk fluid and sessile samples in the control cell. The position of these bands matched the position of the bands in BVI and in BFE profiles. Since DNA can pass freely through a 2 µm filter the bands were representing DNA of dominant bacteria species seeded into the bioreactor vessel. It is important to realize that the presence of the DNA bands alone does not necessarily signify the presence of living bacterial cells. Therefore, it is imperative that molecular data are confirmed with microscopy imaging. SEM results, reported above, verified the absence of bacterial cells in the control flow cell.

Cloning and sequencing confirmed the presence of 16S rRNA sequences characteristic of sulfate-reducing bacteria of the genus *Desulfovibrio* (99% sequence similarity with *Desulfovibrio profunda* DSM 11384) and sulfidogenic spore forming Firmicutes of the genus *Caminiella* (99% sequence homology with *Caminiella sporogenes* strain AM1114) in biofilm field enrichments used for the seeding of the bioreactor vessel (Table 4). However, planktonic and sessile populations in the experimental flow cell revealed H<sub>2</sub>S-producing bacteria of phyla Firmicutes and Synergistetes as dominant clones. In the former phylum, the genus *Caminiella* was the most abundant clone in both, biofilms on steel coupons and in the liquid phase. None of the selected clones had 16S rRNA sequences identifiable as belonging to SRB. Although DNA from SW contained sequences of alphaproteobacteria and bacteria of the genera *Bacillus*, *Rhodobacteriales*, *Oceanospirillates* and *Alteromonas*, there was no evidence that these organisms persisted as dominant species either in the planktonic phase or in biofilms on steel specimens in the experimental flow cell. Sulfidogenic Synergistetes of genera *Thermovirga* and *Anaerobaculum* were identified only in the bulk fluid of the experimental flow cell and were absent in clones from SW and from the bioreactor inoculum.

It is important to note that the selection of clones is a random process. A low abundance of the clone representing certain sequence signifies that DNA representing this sequence is a minor contributor to the overall DNA pool. Therefore, the probability of detecting such sequence is low. The presence of sequences belonging to Synergistetes in the DNA recovered from the liquid phase of the experimental cell and their lack in the bioreactor inoculum and in seawater sample indicates a low frequency of corresponding clones in BVI and in SW DNA samples at the beginning of the experiment. Likewise, the absence of SRB sequences in the experimental flow cell, despite identifying those

**Table 2**  
ICP-AES analysis of corrosion products removed from 6 o'clock positioned steel specimens surface after 100 days of the exposure and dissolved in aqueous HCl solution (50 (v/v)%). Results given in molar concentrations (c(element)/mM) for iron (Fe), calcium (Ca), potassium (K), magnesium (Mg), sodium (Na), and sulfur (S).

	c(Fe)/mM <sup>a</sup>	c(Ca)/mM <sup>b</sup>	c(K)/mM <sup>c</sup>	c(Mg)/mM <sup>d</sup>	c(Na)/mM <sup>e</sup>	c(S)/mM <sup>f</sup>
Control cell	13.9	3.1	0.1	0.3	1.4	0.7
Experimental cell	18.5	1.7	0.1	1.4	1.8	7.3

<sup>a</sup> Molar concentration of iron (Fe) in analyzed sample.

<sup>b</sup> Molar concentration of calcium (Ca) in analyzed sample.

<sup>c</sup> Molar concentration of potassium (K) in analyzed sample.

<sup>d</sup> Molar concentration of magnesium (Mg) in analyzed sample.

<sup>e</sup> Molar concentration of sodium (Na) in analyzed sample.

<sup>f</sup> Molar concentration of sulfur (S) in analyzed sample.

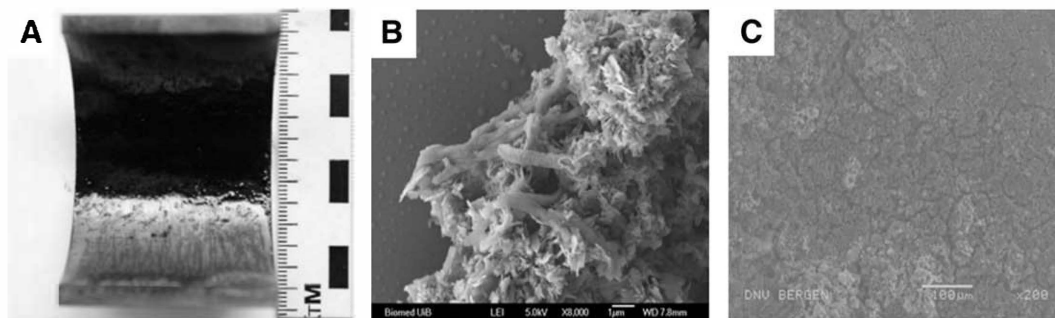


**Fig. 8.** Macro and micro photographs (6 o'clock position) of specimens after 100 days of a exposure in the experimental cell: (A) Photography of coupon before preparation for SEM/EDX; (B) SEM image (8000 $\times$ ) of the immobilized corrosion products/biofilm deposits; (C) SEM image (200 $\times$ ) of black deposit formed in the coupon, total area is scanned by EDX.

sequences in the bioreactor inoculum, is likely due to the increase of DNA from Firmicutes of the class *Clostridia*, of which most are thiosulfate and organic sulphur reducers.

DGGE analysis revealed that bacterial diversity in all DNA samples was higher than the cloning results would indicate. However, as already stated, cloning demonstrated that sulfidogenic spore forming bacterium of the phylum *Firmicutes* and the genus *Caminiella* was, most likely, the dominant biofilm and planktonic organism in the experimental flow cell.

#### 4. Discussion

Corrosion measurements carried out by LPR and EN revealed both similarities and differences in the corrosion behavior of carbon steel specimens exposed in the control cell versus the experimental cell.

The observed initial fluctuations of OCP in both cells were likely reflecting chemical changes to the specimen surfaces occurring during short period after specimen immersion. As mentioned previously, OCP stabilized at  $-800 < E(\text{OCP})/\text{mV}(\text{vs. SCE}) < -700$  in both flow cells which corresponds to values reported elsewhere [53].

For most of the testing period, the overall rate of corrosion, e.g.  $1/(R_p/\Omega)$ , was lower in the experimental flow cell than in the control flow cell. However, at the beginning and towards the end of the experiment, the corrosion behavior was similar in the two cells. In both cells, the corrosion resistance of steel was very high (Fig. 2) during the first 21 days of the test, i.e. before and immediately after inoculation. This indicates that a protective ferrous film remained relatively intact on the metal surface, despite the presence of high concentration of aggressive chloride ions in the seawater. A similarly high corrosion resistance has previously been reported for carbon steel in a sterile artificial growth medium containing high concentrations of aggressive ions [47].

Between day 21 and day 52, there was a marked increase in the  $1/(R_p/\Omega)$  values in the control, but not in the experimental flow cell, see Fig. 2. In general, such variations may be due to differences in the mineralization processes [6,54]. The increase in  $1/(R_p/\Omega)$  for the control flow cell is consistent with a breakdown or a gradual weakening of the protective ferrous layer [54] that occurs concurrently with the observed formation of iron oxides and of a thin, sparse and localized "green rust" layer on the carbon steel surfaces (Fig. 7 and Table 3). Such localized mineral formation has previously been reported to result in increased average  $1/(R_p/\Omega)$  values, presumably due to the formation of galvanic concentration cells [15].

The observation that  $1/(R_p/\Omega)$  remains at relatively low values in the experimental flow cell, up to about day 83, can be given different explanations. It may be that the minerals formed in the experimental flow cell do not have as pronounced an effect of weakening the protective ferrous layer as those formed in the control flow cell. In addition, the presence of biofilm and high concentrations of microbial endo- and exo-metabolites will lead to an additional build-up of a biotic layer on the carbon steel surfaces in the experimental flow cell. Finally, higher concentrations of bacterially produced dihydrogen sulfide in the experimental reactor are expected to result in the formation of different iron sulfides layers (Table 1). Thus, the biotic layer could be modified by a compact and protective layer of iron(II) sulfide (FeS) and iron(III)-oxide (Fe<sub>2</sub>O<sub>3</sub>) [53] or green rust in our study. The evidence is that the cumulative effect of these processes is protective relative to the control cell (Fig. 8).

From about day 50 until test termination, the  $1/(R_p/\Omega)$  values in the control cell remained relatively stable, with some increase, see Fig. 2A. This may reflect a state of instability of surface deposits with opposing rates of formation and destruction of local defects in the corrosion products layers (54). This is supported by the observations of EN pattern characteristics for metastable pitting (Fig. 3A) and of LI values indicative of a mixed corrosion mechanism (Fig. 5A) [48,49].

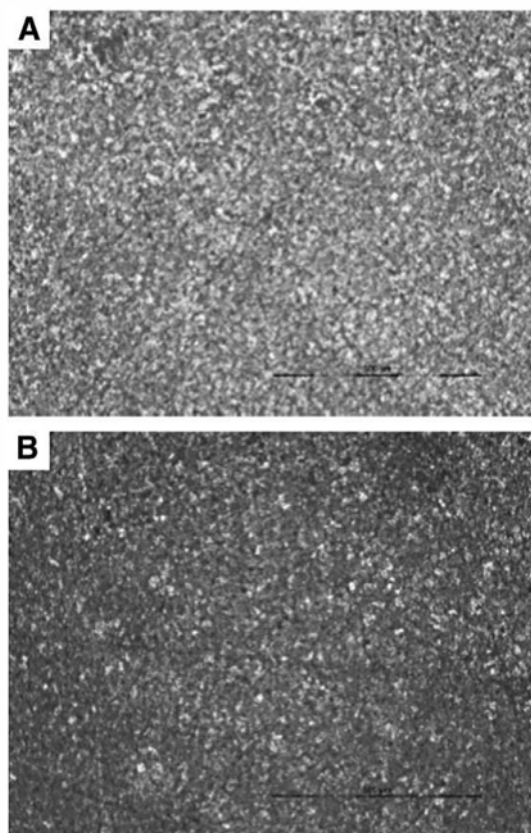


**Fig. 9.** Working electrode micro photographs (100 $\times$ ) after 100 days of an exposure in the: (A) control cell (after corrosion product removal); (B) experimental cell (after corrosion product removal).

**Table 3**

The total number of bands and the number of dominating bands in DGGE profiles in samples with recoverable DNA.

Sample	Number of bands	Number of dominating bands
As-received North Sea seawater (SW)	11	5
The biofilm field enrichment in SRB/2 medium (BFE)	3	2
Bioreactor vessel inoculum (BVI)	7	2
Biofilms from the experimental flow cell (BEFC)	6	2
Water samples from the experimental flow cell (WEFC)	4	1

The EN data suggests a mixed corrosion mechanism for both flow cells. The occurrence of localized corrosion events, in particular metastable pitting, is consistent with the observation of large fluctuation (transients) in the acquired EN data from both flow cells. Conditions favorable for pitting may exist even before reactor inoculation. Sulfate ions may/react with dissolved oxygen (measured at low concentrations during the initial 24 days of the test) to produce aggressive thiosulfate ions [55]. Together with chloride ions, already present at a high concentration in seawater, they create conditions favorable for the onset of localized corrosion events (metastable or stable pitting).

During the course of the experiment, both mineral layers and a microbially-produced protective layer were formed in the experimental flow cell after inoculation, as evidenced by the observation of black deposits comprised of organic matter and mineral corrosion products (Fig. 8B and C). Similar types of deposits have been reported in experiments that involved approximately 125 days of anaerobic stagnant exposure of low carbon steel [53]. In the experiments herein, different minerals were deposited on the surfaces in the control flow cell. All such deposits are likely to modify, to a varying extent, the exposure of the steel surfaces to the aggressive anions and, thus, to induce differences both in corrosion resistance and in the extent of pitting between the two environments.

The breakdown of protective layers and subsequent metastable pitting can occur on metal surfaces without significantly changing

**Table 4**

Identification of bacterial species detected through cloning and sequencing of DNA recovered from field and laboratory samples, including as-received North Sea seawater. Sample description is provided in Section 2.2.4.

Source of DNA	Bacteria identified through cloning and sequencing
SW	Alphaproteobacteria; Rhodobacterales [6] <i>Nautella italica</i> strain LMG 24365 <sup>6</sup> Gammaproteobacteria; Oceanospirillales [1] <i>Alcanivorax dieselolei</i> strain B-5 <sup>5</sup> [10] <i>Alteromonas</i> spp. ( <i>Alteromonas macleodii</i> ) <sup>6</sup> Firmicutes; Bacilli [1] <i>Bacillus smithii</i> strain NRS-173 <sup>4</sup>
BFS	Deltaproteobacteria [4] <i>Desulfovibrio profunda</i> DSM 11384 <sup>1</sup> Marine bacterium [2] <i>Marinitulum fragile</i> strain JC2469 <sup>4,6</sup>
BI	Firmicutes; Clostridia [6] <i>Caminicella sporogenes</i> strain AM1114 <sup>1,2,3,5</sup>
BEFC	Firmicutes; Clostridia [4] <i>Caminicella sporogenes</i> strain AM1114 <sup>1,2,3,5</sup>
WEFC	Firmicutes; Clostridia [5] <i>Caminicella sporogenes</i> strain AM1114 <sup>1,2,3,5</sup> [2] <i>Thermoanaerobacter brockii</i> subsp. <i>Lactiethylicus</i> <sup>1,5</sup> Synergistetes [1] <i>Thermovirga lienii</i> DSM 17291 strain Cas60314 <sup>1,2,3,5</sup> [2] <i>Anaerobaculum thermoterrnum</i> strain RWcit <sup>1,5</sup>

[x] Number of clones.

Physiology: <sup>1</sup>H<sub>2</sub>S production, <sup>2</sup>Acetate production, <sup>3</sup>H<sub>2</sub> production, <sup>4</sup>Nitrate reduction, <sup>5</sup>Thermophilic and <sup>6</sup>Mesophilic.

the corrosion resistance. This has been reported, for example, for SRB harboring marine biofilms [53].

In the experimental flow cell, a substantial increase in corrosion rate was recorded after 92 days of testing. This was likely caused by a breakdown of an iron sulfide layer, most probably induced by minor changes to the chemistry of the environment, such as a decrease of pH.

The presence of both calcium and magnesium mineral deposits in flow cells indicate the possible precipitation of carbonates, including an iron-dolomite mineral, e.g. Fe-CaMg(CO<sub>3</sub>)<sub>2</sub>. Dolomite formation is generally observed at high temperatures; however, it has also been described at low temperature [56,57]. Development of dolomite under anaerobic sulfidogenic conditions has been reported in Lagoa Vermelha and Brejo do Espinho, two supersaturated saline lagoons along the Rio de Janeiro coast of Brazil [56–58]. Sulfide-producing Firmicutes e.g. *Caminicella* specie, identified as dominant biofilm and planktonic organism in the experimental cell, generates, as reported for many clostridia, high concentrations of carbon dioxide during its growth. The combination of anoxic production of carbon dioxide and sulfide ions would facilitate precipitation of carbonate minerals. It is widely accepted that, if intact, calcareous deposits on steel surfaces act as a protective barrier against chloride and sulfide anions.

Identification of Firmicutes as a dominant phylum in analyzed biofilms was not surprising. They are ubiquitous in marine environments and *Clostridia* are typically more versatile in the use of carbon sources and electron donors/acceptors than SRB. It is most likely that under favorable growth conditions, *Clostridia* outcompete SRB in biofilms on carbon steel. Moreover, presence of sulfidogenic microorganisms other than SRP was expected due to nature of the growth media used for preparing inoculates. The commercial SRB/2 media used for preparing biofilm field enrichments are also selective for dihydrogen sulfide producers other than SRP. A number of reports indicate that the spore forming sulfidogenic and carbon dioxide producing populations representing *Clostridia* are very abundant in oil field systems, frequently outnumbering SRP [10,30,59]. It is, thus, conceivable that this group of bacteria poses higher corrosion and souring threat to oilfield installations than SRB alone.

Moreover, the general corrosion deterioration pattern revealed after corrosion product removal in both cells confirms the EN analysis regarding type of corrosion mechanism that took place on exposed surfaces (mixed mechanism; pitting/general corrosion). It is noteworthy that the uniform corrosion can result from the merging of continuously formed stable and metastable pits [60].

The observed final corrosion rate of carbon steel was relatively moderate, irrespective of whether the steel was exposed to seawater or to a combination of seawater and sulfidogenic bacterial community. Corrosion rates of carbon steel observed at the end of the 100 day test period in bioreactor flow loop were in agreement with integrity evaluations (corrosion rates acquired by electric resistance (ER) and LPR probes) of low carbon steel SWIS located on an offshore installation in the Norwegian sector of the North Sea (personal communication). It is required to keep in mind that even though acquired corrosion rate values are very similar, it is possible that in a more appropriate experimental set-up (continuously fed with fresh media flow loop enabling higher fluid velocities would be more representative of typical SWIS) acquired values could differ more depending on the presence and activity of biofilms. It was reported that the amount of nutrients, possibly limited by experimental set-up volume in this investigation, may be the restricting factor for microbial activity [16], as well as a factor inhibiting electrochemical activity of established biofilms [36]. Therefore, lack of sufficient amount of nutrients may result with lower corrosion rates in systems where main culprits of corrosion are bacteria. Even though the bioreactor loop accommodated relatively low volume of test media (approximately 40 L), same volume was sufficient for development of electroactive biofilms that led to relatively low corrosion and formation of specific bioinorganic and corrosion products. Longer exposure periods could lead to elevated corrosion rates. However, the

100-day test is relevant as it represents typical period between two pigging operations (cleaning operations) and time between replacements of offshore electrochemical probes.

A number of studies address corrosion of carbon steel, and thus the evolution of carbon steel integrity, in laboratory experiments in which the carbon steel was exposed to pure sulfidogenic cultures or to isolated offshore consortia in different growth media [47,61,62]. Additional reports have presented results on long-term exposures of structural steel in natural seawater [63]. Mostly, low corrosion rates and the presence of mixed corrosion mechanisms were reported [47,61]. These results are in good agreement with the outcome of the present investigation.

## 5. Conclusion

Our current work has shown that under chosen experimental conditions, metabolic activity of sessile sulfide and carbon dioxide producing bacterial populations dominated by *Caminiella* specie generated abundant sulfide layer, as well as carbonaceous mineral precipitates on the carbon steel samples. The overall impact of the bacterial consortium on the corrosion rate of S235JR carbon steel specimens was minor. The sterile/inoculated condition had apparently no significant influence on the corrosion rate of carbon steel during the 100 days of exposure in the flow reactors. Clearly, the release of biogenic sulfide does not necessarily lead to extensive localized pitting attack. It is apparent that metabolic activities of cells are likely to influence the chemistry of bioinorganic corrosion products and should be considered when evaluating MIC risk.

It is worth mentioning that despite offering valuable insights into complex corrosion processes occurring in biotic systems, strictly controlled laboratory tests are not totally representative for offshore water injection systems. Therefore, before implementing with confidence these findings into the corrosion monitoring routines of the oil and gas industry, it is important to evaluate in-depth all differences between the laboratory and field corrosion measuring methodologies. A perfect alignment of the laboratory and field corrosion data would ensure immediately field-applicable corrosion control measure.

## Acknowledgments

Funding was received from the European Community's Seventh Framework Programme (FP7/2007-2013). The authors wish to express their gratitude towards Dr. Jan Sunner from University of Oklahoma, Dr. Karine Drønen from University of Bergen, and Ing. Øystein Birketveit from MISWACO for their support in the production of the presented work.

## References

- [1] S.W. Borenshtein, *Microbiologically Influenced Corrosion Handbook*, Woodhead Publishing Limited, Cambridge, UK, 1994.
- [2] H.A. Videla, *Manual of Biocorrosion*, CRC Press, Boca Raton, FL, USA, 1996.
- [3] In: E. Heitz, H.C. Flemming, W. Sand (Eds.), *Microbially Influenced Corrosion of Materials*, Springer-Verlag GmbH & Co KG, Berlin, Germany, 1996.
- [4] I.B. Beech, J. Sunner, *Biocorrosion: towards understanding interactions between biofilms and metals*, *Curr. Opin. Biotechnol.* 15 (2004) 181–186.
- [5] M. Madigan, J.M. Martinko, P.V. Dunlap, D.P. Clark, *Brock Biology of Microorganisms*, 13th ed. Pearson-Benjamin Cummings, San Francisco, CA, USA, 2012.
- [6] J. Duana, S. Wua, X. Zhanga, G. Huangb, M. Duc, B. Houa, *Corrosion of carbon steel influenced by anaerobic biofilm in natural seawater*, *Electrochim. Acta* 54 (2008) 22–28.
- [7] M. Franklin, D.C. White, B.J. Little, R. Ray, R. Pope, *The role of bacteria in pit propagation of carbon steel*, *Biofouling* 15 (2000) 13–23.
- [8] A. Agrawal, K. Vanbroekhoven, B. Lal, *Diversity of culturable sulfidogenic bacteria in two oil–water separation tanks in the north-eastern oil fields of India*, *Anaerobe* 16 (2010) 12–18.
- [9] J. Jan-Roblero, J.M. Romero, M. Amaya, S. Le Borgne, *Phylogenetic characterisation of a corrosive consortium isolated from a sour gas pipeline*, *Appl. Microbiol. Biotechnol.* 64 (2004) 862–867.

- [10] H.S. Park, I. Chatterjee, X. Dong, S.-H. Wang, C.W. Sensen, S.M. Caffrey, et al., *Effect of sodium bisulfite injection on the microbial community composition in a brackish-water-transporting pipeline*, *Appl. Environ. Microbiol.* 77 (2011) 6908–6917.
- [11] J. Larsen, K. Rasmussen, H. Pedersen, K. Sørensen, T. Lundgaard, T.L. Skovhus, *Consortia of MIC bacteria and archaea causing pitting corrosion in top side oil production facilities*, *Corrosion/2010*, Paper no. 10252, NACE International, San Antonio, TX, 2010.
- [12] T. Zhang, H.H. Fang, B.C. Ko, *Methanogen population in a marine biofilm corrosive to mild steel*, *Appl. Microbiol. Biotechnol.* 63 (2003) 101–106.
- [13] S.M. Caffrey, H.S. Park, J. Been, P. Gordon, C.W. Sensen, G. Voordouw, *Gene expression by the sulfate-reducing bacterium *Desulfovibrio vulgaris* Hildenborough grown on an iron electrode under cathodic protection conditions*, *Appl. Environ. Microbiol.* 74 (8) (2008) 2404–2413.
- [14] R.E. Melchers, R. Jeffrey, *The critical involvement of anaerobic bacterial activity in modeling the corrosion behavior of mild steel in marine environments*, *Electrochim. Acta*, 542008. 80–85 (Special Issue BIOCORROSION OF MATERIALS).
- [15] B.J. Little, J.S. Lee, *Microbiologically Influenced Corrosion*, Hoboken, John Wiley and Sons Inc., New Jersey, USA, 2007.
- [16] K. Pedersen, *Factors regulating microbial biofilm development in a system with slowly flowing seawater*, *Appl. Environ. Microbiol.* 44 (5) (1982) 1196–1204.
- [17] P. Lens, V. O'Flaherty, A.P. Moran, P. Stoodley, T. Mahony, *Biofilms in Medicine Industry and Environmental Biotechnology*, IWA Publishing, London, UK, 2003. 121–124.
- [18] K.F. Ettwig, D.R. Speth, J. Reimann, M.L. Wu, M.S.M. Jettenand, J.T. Keltjens, *Bacterial oxygen production in the dark*, *Evolutionary and Genomic Microbiology*, *Frontiers in Microbiology*, 3, August 3 2012, (Article 273).
- [19] J.D. Coates, R.T. Anderson, *Emerging techniques for anaerobic bioremediation of contaminated environments*, *Trends Biotechnol.* 18 (10) (2000) 408–412.
- [20] T. Richardson, R.A. Cottis, R. Lindsay, S. Lyon, D. Scantlebury, H. Stott, et al., *Shreir's Corrosion 2010: Corrosion in Microbial Environments*, vol. 2, Elsevier, Oxford, UK, 2010.
- [21] J. Wen, K. Zhao, T. Gu, S. Nešić, *Effects of mass transfer and flow conditions on SRB corrosion of mild steel*, *Corrosion/2006*, Paper No. 06666, NACE International, Houston, TX, 2006.
- [22] P. Stoodley, I. Dodds, J.D. Boyle, H.M. Lappin-Scott, *Influence of hydrodynamics and nutrients on biofilm structure*, *J. Appl. Microbiol. Symp. Suppl.* 85 (28) (1999) 19–28.
- [23] J. Wen, T. Gu, S. Nešić, *Investigation of the effects of fluid flow on SRB biofilm*, *Corrosion/2007*, Paper No. 07516, NACE International, Nashville, TN, 2007.
- [24] W. Teughels, N. Van Assche, I. Sliepen, M. Quirynen, *Effect of material characteristics and/or surface topography on biofilm development*, *Clin. Oral Implants Res.* 17 (2006) 68–81.
- [25] D. Clover, B. Kinsella, B. Pejčić, R. De Marco, *The influence of microstructure on the corrosion rate of various carbon steels*, *J. Appl. Electrochem.* 35 (2005) 139–149.
- [26] R. Cord-Rustwisch, W. Kleinitz, F. Widdel, *Sulfate-reducing bacteria and their activities in oil production*, *J. Pet. Technol.* 39 (1) (1987) 97–106.
- [27] J. Larsen, K. Sørensen, K. Højris, T.L. Skovhus, *Significance of troublesome sulfate-reducing prokaryotes (SRP) in oil field systems*, *Corrosion/2007*, Paper No. 09389, NACE International, Atlanta, GA, 2009.
- [28] J.M. Sufliita, D.F. Aktas, A.L. Oldham, B.M. Perez-Ibarra, K.E. Duncan, *Molecular tools to track bacteria responsible for fuel deterioration and microbiologically influenced corrosion*, *Biofouling* 28 (9) (2012) 1003–1010.
- [29] D. Li, D.J. Midgley, J.P. Ross, Y. Oytam, G.C.J. Abell, H. Volk, et al., *Microbial biodiversity in a Malaysian oil field and a systematic comparison with oil reservoirs worldwide*, *Arch. Microbiol.* 194 (6) (2012) 513–523.
- [30] E. Korenblum, É. Valoni, M. Penna, L. Seldin, *Bacterial diversity in water injection systems of Brazilian offshore oil platforms*, *Appl. Microbiol. Biotechnol.* 85 (2010) 791–800.
- [31] K.E. Duncan, L.M. Gieg, V.A. Parisi, R.S. Tanner, S.G. Tringe, J. Bristow, et al., *Biocorrosive thermophilic microbial communities in Alaskan North Slope oil facilities*, *Environ. Sci. Technol.* 43 (2009) 7977–7984.
- [32] A. Rajasekar, B. Anandkumar, S. Maruthamuthu, Y.-P. Ting, P.K.S.M. Rahman, *Characterization of corrosive bacterial consortia isolated from petroleum-product-transporting pipelines*, *Appl. Microbiol. Biotechnol.* 85 (2010) 1175–1188.
- [33] R.D. Kane, *Control of microbially induced corrosion in seawater*, *Corrosion/2004*, Paper No. 04579, NACE International, Houston, TX, 2004.
- [34] G.J. Licina, C.S. Carney, *Monitoring biofilm formation and incipient MIC in real time*, Paper No. 175, *Corrosion/99*, NACE International, Houston, TX, 1999.
- [35] J. Lin, J.R. Frank, E.J. St. Martin, D.H. Pope, *Electrochemical noise measurements of sustained microbially influenced pitting corrosion in a laboratory flow loop system*, Paper No. 198, *Corrosion/99*, NACE International, Houston, TX, 1999.
- [36] M. Faimali, E. Chelossi, G. Pavanello, A. Benedetti, I. Vandecastelaere, P. De Vos, et al., *Electrochemical activity and bacterial diversity of natural marine biofilm in laboratory closed-systems*, *Bioelectrochemistry* 78 (2010) 30–38.
- [37] American Petroleum Institute, *API-RP 348*, 1990.
- [38] F. Widdel, G.W. Kohring, F. Mayer, *Studies on dissimilatory sulfate-reducing bacteria that decompose fatty acids. 111. Characterization of the filamentous gliding *Desulfonema limicola**, *Microbiology* 134 (1983) 286–294.
- [39] M. Stern, A.L. Geary, *Electrochemical polarization. I. A theoretical analysis of the shape of the polarization curves*, *J. Electrochem. Soc.* 104 (1957) 56–63.
- [40] M. Stern, *A method for determining corrosion rates from linear polarization data*, *Corrosion* 14 (9) (1958) 440–444.
- [41] R.A. Cottis, S. Turgoose, *Electrochemical impedance and noise*, in: Barry C. Syrett (Ed.), *Corrosion Testing Made Easy Series*, NACE International, Houston, 1999.
- [42] D.A. Eden, *Electrochemical noise — The first two octaves*, *Corrosion/98*, Paper No. 386, NACE International, Houston, TX, 1998.

- [43] S.A. Reid, D.A. Eden, Assessment of Corrosion, patent no.: US 6.264.824 B1, United States Patent (2001).
- [44] G. Muyzer, T. Brinkhoff, U. Nubel, C. Santegoeds, H. Schafer, C. Wawer, Denaturing gradient gel electrophoresis (DGGE) in microbial ecology, *Mol. Microb. Ecol. Man.* (1998) 1–27.
- [45] J. Sambrook, E.F. Fritsch, T. Maniatis, Analysis and cloning of eukaryotic genomic DNA, molecular cloning: a laboratory manual, 9, Cold Spring Harbor Laboratory Press, Cold Spring Harbor, NY, 1989, pp. 45–46.
- [46] J. Messing, R. Crea, P.H. Seeburg, A system for shotgun DNA sequencing, *Nucleic Acids Res.* 9 (1981) 309–314.
- [47] A. Padilla-Viveros, E. Garcia-Ochoa, D. Alazard, Comparative electrochemical noise study of the corrosion process of carbon steel by the sulfate-reducing bacterium *Desulfovibrio alaskensis* under nutritionally rich and oligotrophic culture conditions, *Electrochim. Acta* 51 (2006) 3841–3847.
- [48] X. Jiang, S. Nešić, Electrochemical investigation of the role of  $\text{Cl}^-$  on localized  $\text{CO}_2$  corrosion of mild steel, 17th International Corrosion Congress, Paper No. 2414, Las Vegas, NV, 2008.
- [49] C.C. Arteaga, J.P. Calderón, C.F. Campos Sedano, J.A. Rodríguez, Comparison of corrosion resistance of carbon steel and some stainless steels exposed to  $\text{LiBr-H}_2\text{O}$  solution at low temperatures, *Int. J. Electrochem. Sci.* 7 (2012) 445–470.
- [50] A. Zegeye, L. Huguet, M. Abdelmoula, C. Carterret, M. Mullet, F. Jorandet, Biogenic hydroxysulfate green rust, a potential electron acceptor for SRB activity, *Geochim. Cosmochim. Acta* 71 (22) (2007) 5450–5462.
- [51] Stefan Krause, Volker Liebetrau, Stanislav Gorb, Mónica Sánchez-Román, Judith A. McKenzie, Tina Treude, Microbial nucleation of Mg-rich dolomite in exopolymeric substances under anoxic modern seawater salinity: New insight into an old enigma, *Geology* 40 (2012) 587–590.
- [52] S.B. Mukkamala, C.E. Anson, A.K. Powell, Modelling calcium carbonate biomineralisation processes, *J. Inorg. Biochem.* 100 (2006) 1128–1138.
- [53] J.S. Lee, R.I. Ray, E.J. Lemieux, M.N. Tamburri, B.J. Little, An evaluation of carbon steel corrosion under stagnant seawater conditions, *Corrosion/2004*, Paper No. 04595, NACE International, Houston, 2004.
- [54] H.A. Videla, L.K. Herrera, R.G. Edyvean, An updated overview of SRB influenced corrosion and protection of carbon steel, *Corrosion/2005*, Paper No. 05488, NACE International, Houston, TX, 2005.
- [55] H.A. Videla, C. Swords, R.G.J. Edyven, Marine Corrosion in Tropical Environments, American Society for Testing and Materials, 2000, 272.
- [56] C. Vasconcelos, J.A. McKenzie, S. Bernasconi, D. Grujic, A.J. Tien, Microbial mediation as a possible mechanism for natural dolomite formation at low temperature, *Nature* 337 (1995) 220–222.
- [57] R. Warthmann, Y. van Lith, C. Vasconcelos, J.A. McKenzie, A.M. Karpoff, Bacterially induced dolomite precipitation in anoxic culture experiments, *Geology* 28 (2000) 1091–1094.
- [58] Y. van Lith, C. Vasconcelos, R. Warthmann, J.C.F. Martins, J.A. McKenzie, Bacterial sulfate reduction and salinity: two controls on dolomite precipitation in Lagoa Vermelha and Brejo do Espinho (Brazil), *Hydrobiologia* 485 (2002) 35–49.
- [59] B.S. Stevenson, H.S. Drilling, P.A. Lawson, K.E. Duncan, V.A. Parisi, J.M. Sufliata, Microbial communities in bulk fluids and biofilms of an oil facility have similar composition but different structure, *Environ. Microbiol.* 13 (2011) 1078–1090.
- [60] R. Jeffrey, R.E. Melchers, The changing topography of corroding mild steel surfaces in seawater, *Corros. Sci.* 49 (2007) 2270–2288.
- [61] W. Lee, W.G. Characklis, Corrosion of mild steel under anaerobic biofilm, *Corrosion* 49 (3) (1998) 197–199.
- [62] M.J. Hernández Gayosso, G. Zavala Olivares, N. Ruiz Ordaz, C. Juárez Ramirez, R. García Esquivel, A. Padilla Viveros, Microbial consortium influence upon steel corrosion rate, using polarization resistance and electrochemical noise techniques, *Electrochim. Acta* 49 (2004) 4295–4301.
- [63] C.R. Southwell, Influence of Marine Organisms on the Life of Structural Steel in Seawater, Naval Research Laboratory, Washington, D.C, 1974.

**Marko Stipanicev** received his M.Sc. degree from the Faculty of chemical engineering and technology, University of Zagreb, Croatia in 2009. He started in 2010 an engineering and research career with Det Norske Veritas in Norway within a Marie Curie Initial Training Network (ITN), BIOCOR. He is enrolled in PhD program MEGeP, University of Toulouse, France in 2011. His current work is dedicated to biocorrosion, with emphasis on more reliable monitoring and decision support for offshore O&G operators.

**Florin Turcu** earned a PhD in Analytical Chemistry from the Ruhr University Bochum, Germany. He is author or co-author of 12 papers published in peer-reviewed journals and has 22 contributions to various international conferences. After a short research stage at the Max Planck Institute for Iron Research, he started in 2007 an engineering career with Det Norske Veritas in Norway. His current work is dedicated to corrosion including laboratory testing, field examinations, and qualification of new technologies.

**Loic Esnault** obtained a Bachelor's Degree in Microbiology from the University of Paris 6 "Pierre et Marie Curie" in 2005, a Master's Degree in Environmental Engineering and Materials Science from National School of Bridge and Road (ENPC) in 2007, and a Doctorate in Geoscience and in biogeochemistry from Nancy University in 2010. His research area is focused on integrity of materials and their behavior in environmental conditions with an innovating specialization in taking into account microbiological reactivity.

**Omar Rosas Camacho** obtained his PhD in Materials Science and Engineering from The Pennsylvania State University in 2010 investigating the corrosion of low carbon steel by carbon dioxide in presence of organic acids. Omar worked on modeling the passivation of low carbon steel in alkaline media and for the last two years, he participated in BIOCOR-ITN investigating the effect of iron reducing bacteria and wild strain from the water injection systems in the corrosion of carbon steel. Currently, Omar is a Research Associate for the National Center for Education and Research in Corrosion and Materials Performance in the University of Akron in USA.

**Dr. Régine Basséguy**, CNRS senior scientist at the Laboratoire de Génie Chimique (LGC, Toulouse – France), specialized in interfaces conductive material/biological system (from enzyme to biofilm), coordinator of French Research Programs, Coordinator of the Marie Curie Network 'BIOCOR ITN' (grant agreement n°238579), Vice-Chairman of the Working Party 10 Microbial Corrosion of the European Federation of Corrosion (EFC), Co-author of 35 publications in International Reviews, 4 patents and 3 Invited conferences.

**Magdalena K. Sztylek** received her M.Sc. degree in biotechnology from the Medical University of Silesia, Poland in 2009. She is a PhD student in the School of Pharmacy and Biomedical Sciences at University of Portsmouth, UK within a Marie Curie Initial Training Network (ITN), BIOCOR. Her PhD project is in the area of development of biochip for biocorrosion monitoring.

**Iwona B. Beech** holds MSc degrees in Physics from the Technical University of Warsaw, Poland, in Plant Pathology from the Imperial College, University of London and PhD in Microbiology from the University of Central London. Her expertise and extensive experience in multi- and inter-disciplinary biofilm and biocorrosion research is evidenced by over 110 publications in peer-reviewed journals. While the University of Portsmouth in the UK is her home institution, she is currently on a leave of absence and employed as a full research professor and a member of the Biocorrosion Center at the University of Oklahoma in Norman, USA.